nature communications

Article

https://doi.org/10.1038/s41467-025-64048-z

An NLR pair in the *Pm68* locus confers powdery mildew resistance in durum and common wheat

Received: 14 December 2024

Accepted: 6 September 2025

Published online: 10 October 2025

Check for updates

Huagang He[1] ✉, Qiulian Tang[1], Qianyuan Zhang[1], Shanying Zhu[2], Sijia Lv[3], Yinguang Bao[4], Jiabao Liang[5], Jiale Wang[1], Jin Wang[1], Hongxing Xu[3], Emile Cavalet-Giorsa[6], Simon G. Krattinger[6], Hongjie Li[7], Chundu Wu[2], Anli Gao[3] ✉ & Yajun Wang[5] ✉

Common wheat and durum wheat are widely cultivated cereal crops, both of which are infected by the obligate biotrophic pathogen *Blumeria graminis* f. sp. *tritici* (*Bgt*), causing powdery mildew. Recently, *Pm68* gene was identified on the short arm of chromosome 2B in the Greek durum wheat line TRI 1796, conferring resistance to this disease. Here, we have cloned *Pm68* from TRI 1796 using an integrated approach of genetic mapping, association analysis and PacBio sequencing. Transgenic assays demonstrate that *Pm68* mediated resistance is controlled by a pair of genetically linked nucleotide-binding leucine-rich repeat (NLR)-encoding genes, *Pm68-1* and *Pm68-2*. Transient expression assays in *Nicotiana benthamiana* leaves reveal that the activation of Pm68-1 is positively modulated by Pm68-2, likely through its N-terminal coiled-coil (CC)-like domain. Evolutionary analysis traces the origin of *Pm68* to a specific wild emmer subpopulation. The introgression and transgenic wheat lines carrying this gene show no significant negative effects on major agronomic traits, highlighting the potential value of *Pm68* for disease-resistant breeding programs of both durum wheat and common wheat.

Common wheat (*Triticum aestivum* L., $2n = 6x = 42$, AABBDD) and durum wheat (*T. turgidum* subsp. *durum* Desf. Husn., $2n = 4x = 28$, AABB) are two related species with distinct grain properties and end-use purposes. Common wheat is globally cultivated and contributes approximately 18% of the calories consumed by humans[1]. Durum wheat, on the other hand, is cultivated in a more limited range of agricultural regions and its grains are mainly used to make pasta[2]. Both common and durum wheat productions are frequently challenged by various fungal diseases, including powdery mildew, rusts, and *Fusarium* head blight. Powdery mildew, a foliar disease caused by the obligate biotrophic pathogen *Blumeria graminis* f. sp. *tritici* (*Bgt*), is prevalent in most wheat-growing regions worldwide, resulting in significant yield losses and posing a threat to global food security[3,4].

The mining and utilization of powdery mildew resistance (*Pm*) genes are crucial for the management of powdery mildew of common wheat and durum wheat. More than 100 *Pm* genes/alleles have been characterized from wheat and its relatives[5,6]. Up to now, 24 *Pm* genes have been cloned, including *Pm1a*[7], *Pm2*[8], *Pm3*[9], *Pm4*[10], *Pm5e*[11], *Pm8*[12], *Pm12*[13], *Pm13*[4,14], *Pm17*[15], *Pm21*[16], *Pm24*[17], *Pm26*[18], *Pm36*[19], *Pm38/Yr18/Lr34/Sr57*[20], *Pm41*[21], *Pm46/Yr46/Lr67/Sr55*[22], *Pm55*[23], *Pm57*[24], *Pm60*[25],

[1]School of Life Sciences, Jiangsu University, Zhenjiang, China. [2]School of Environment and Safety Engineering, Jiangsu University, Zhenjiang, China. [3]School of Life Sciences, Henan University, Kaifeng, China. [4]College of Agronomy, Shandong Agricultural University, Taian, China. [5]State Key Laboratory of Plant Trait Design, CAS Centre for Excellence in Molecular Plant Sciences, Shanghai Institute of Plant Physiology and Ecology, Chinese Academy of Sciences, Shanghai, China. [6]Plant Science Program, Biological and Environmental Science and Engineering Division, King Abdullah University of Science and Technology (KAUST), Thuwal, Saudi Arabia. [7]Institute of Biotechnology, Xianghu Laboratory, Hangzhou, China. ✉e-mail: hghe@ujs.edu.cn; algao@henu.edu.cn; yjwang@cemps.ac.cn

Pm69[26], *WTK4*[27], *PmTR1*[28], *Pm6Sl*[29] and *PmAeu1*[30]. Among them, 15 genes encode coiled coil nucleotide-binding leucine-rich-repeat (NLR) proteins, while the others encode kinase fusion proteins (KFPs) or multi-transmembrane transporters[18,31–33].

Four designated *Bgt* resistance loci have been identified in durum wheat. *Mld* is a recessive gene on chromosome 4B that has lost its effectiveness[34]. *Pm3h* is a dominant gene on chromosome 1AS of an Ethiopian durum wheat accession[35], whose sequence is identical to *Pm3d*[36]. *PmDR147* is a dominant gene on 2AL of durum wheat accession DR147[37]. *Pm68* was identified in the Greek durum wheat accession TRI 1796. Through bulked segregant RNA-Seq (BSR-Seq) analysis combined with genetic mapping using a bi-parent population, *Pm68* was mapped to a 0.44-cM genetic interval on the terminal part of chromosome arm 2BS, corresponding to a 1.78-Mb physical region of the reference genome of durum wheat cv. Svevo[38]. Durum wheat accession TRI 1796 is highly resistant to all 22 tested *Bgt* isolates, suggesting that this gene has potential for powdery mildew resistance breeding in both durum wheat and common wheat.

In this study, we report the cloning of *Pm68* from durum wheat using a strategy that combines genetic fine mapping, association analysis and PacBio sequencing. *Pm68* resistance is mediated by the NLR pair *Pm68-1* and *Pm68-2*. *Pm68-1* encodes a canonical NLR containing a coiled-coil (CC) domain, a nucleotide-binding site (NBS) domain and a leucine-rich repeat (LRR) domain, whereas *Pm68-2*-encoded NLR lacks a typical CC domain but possesses a four-helix bundle structurally analogous to a CC domain, designated here as a CC-like (CC_l) domain. Transgenic plants expressing either *Pm68-1* or *Pm68-2* are susceptible to powdery mildew, while hybrid F_1 and F_4 carrying the two NLRs are all resistant. Transient over-expression analyses in *Nicotiana benthamiana* leaves indicate that Pm68-1 plays a critical role in triggering cell death, which is regulated by Pm68-2, likely through its N-terminal CC_l domain. The *Pm68*-carrying chromosome segment could be traced to a genetically distinct and geographically restricted wild emmer subpopulation. We have transferred *Pm68* into the elite common wheat cultivar Yangmai 158 (YM158) by interspecific hybridization. In both common wheat introgression lines and transgenic lines expressing *Pm68*, no significant deleterious effects on major agronomic traits were observed, suggesting that *Pm68* has a potential value for common wheat and durum wheat breeding.

Results

Pm68 is delimited to 266-kb and 297-kb regions corresponding to Svevo and Zavitan reference genomes, respectively

For genetic fine mapping of *Pm68*, the previously identified flanking markers *Xdw03* and *Xdw15* were used to screen 1382 F_2 individuals derived from the cross between durum wheat accessions TRI 1796 (resistant) and PI 584832 (susceptible). A total of 41 recombinants were obtained and then further genotyped using another 8 co-dominant markers (Supplementary Data 1 and 2). As a result, *Pm68* was mapped to a 0.21-cM genetic interval flanked by markers *Xdw05/Xdw06* and *Xdw09/Xdw10* corresponding to a 434-kb region in the reference genome of durum wheat cv. Svevo[39]. Three markers *Xdw07*, *Xdw08* and *Xdw08.9* co-segregated with *Pm68* (Fig. 1a).

To further narrow the *Pm68* locus, we inoculated 120 durum wheat accessions with *Bgt* iaolate BgtYZ01 at the one-leaf stage. As a result, 114 accessions displayed highly susceptible phenotypes (IT 4), while 6 accessions (including TRI 1796) showed resistance with hypersensitive reactions (HR) (IT 0;) which resembles *Pm68*-mediated resistance (Supplementary Fig. 1; Supplementary Data 3). We then genotyped the above six resistant and 85 susceptible durum wheat accessions using 7 co-dominant markers (*Xdw05* – *Xdw10* and *Xdw8.9*) spanning the *Pm68* locus. *Xdw07* and *Xdw08* showed segregation with *Pm68*, left *Xdw08.9* was the only marker co-segregated with *Pm68* both in F_2 and association mapping populations (Fig.1a, b; Supplementary Data 2 and 4). Therefore, *Pm68* was mapped to region flanked by markers *Xdw08* and *Xdw09*, corresponding to a 266-kb and a 297-kb physical intervals of durum wheat Svevo[39] and wild emmer Zavitan[40] reference genomes, respectively (Fig.1c).

The *Pm68*-mediated resistance to powdery mildew is controlled by a pair of NLR genes

The 266-kb *Pm68* interval of Svevo reference genome contains 15 annotated genes, while the corresponding 297-kb Zavitan interval contains 7 annotated genes (Fig.1c). Eight gene-derived markers (*Xdw08.1* – *Xdw08.8*) were developed from five Svevo genes and three Zavitan genes, which were used to genotype the two parents, TRI 1796 and PI 584832. We found that five Svevo gene-derived markers (*Xdw08.1* – *Xdw08.5*) only amplified from the susceptible parent PI 584832, while three Zavitan gene-derived markers (*Xdw08.6* – *Xdw08.8*) only amplified from resistant parent TRI 1796 (Supplementary Fig. 2a), suggesting that TRI 1796 harbors a haplotype similar to wild emmer Zavitan, rather than durum wheat Svevo (Fig. 1c).

Since Zavitan exhibited a susceptible phenotype (IT 4) to *Bgt* isolate BgtYZ01 (Supplementary Fig. 3), we sequenced the genome of the *Pm68* donor accession TRI 1796 using the PacBio circular consensus sequencing (CCS) platform and obtained 5,571,107 HiFi reads consisting of ~98 Gb genomic sequence data, approximately 9.4-fold coverage of Svevo genome (10.45 Gb) and 9.7-fold coverage of Zavitan genome (10.1 Gb). After sequence assembling, 11,467 contigs were obtained, with a contig N50 of 1.78 Mb and N90 of 0.52 Mb, and a total length of the assembly of 10.41 Gb. The flanking markers *Xdw08* and *Xdw09* were positioned on a single 4.46-Mb contig ptg004078l. Dot plot analyses revealed that the *Pm68* interval of TRI 1716 is highly similar to Zavitan and diverged from Svevo (Supplementary Fig. 2b). The *Xdw08* and *Xdw09* flanked 305-kb TRI 1716 interval corresponds to 297-kb region of Zavitan genome, and the seven annotated genes from Zavitan interval also align to seven corresponding alleles from TRI 1716 (Fig. 1d).

To identify causal gene(s) of *Pm68*, we mapped RNA-seq reads from BgtYZ01-infected TRI 1716 leaf tissues to the TRI 1716 genome assembly. Four out of the seven annotated genes, including *TRIDC2BG003960*, *TRIDC2BG003970*, *TRIDC2BG003990* and *TRIDC2BG004000*, were found to have relatively high read-mapping depth, while no reads mapped to the rest three genes, *TRIDC2BG003940*, *TRIDC2BG003950* and *TRIDC2BG003980* (Fig. 1d). This indicated that only four genes out the seven were expressed in BgtYZ01- infected TRI 1716 leaf tissues. Among these four expressed genes, *TRIDC2BG003970* and *TRIDC2BG003990* encode two NLR receptors, *TRIDC2BG004000* encodes a U4/U6 small nuclear ribonucleoprotein Prp31, and *TRIDC2BG003960* encodes an unknown function protein with no annotated conserved domain. Given that NLR genes are often responsible for disease resistance, the TRI 1796 genes corresponding to *TRIDC2BG003970* and *TRIDC2BG003990* in Zavitian were considered as the most likely the candidates for *Pm68*, and referred as *Pm68-1* and *Pm68-2* hereafter (Fig. 1d). Both NLR genes contain no introns and are arranged in a head-to-head orientation, 202 kb apart in the TRI 1796 genome. The qRT-PCR assay validated the expression of *Pm68-1* and *Pm68-2*, and their transcript levels were not induced by *Bgt* infection (Supplementary Fig. 4). Sequence comparison of these two NLRs demonstrated that both resistant TRI 1796 and susceptible Zavitan have an identical *Pm68-1* coding sequence (CDS) (2742 bp), but differ from one nucleotide in their *Pm68-2* CDS (G1111T), leading to a premature stop codon in the *Pm68-2* allele from Zavitan (Fig. 1d). As Zavitan is susceptible to BgtYZ01, it was suggested that a functional *Pm68-2* is necessary for *Pm68* resistance.

We amplified the full-length coding regions of *Pm68-1* and *Pm68-2*, and separately ligated them into the vector pLGY02 with an expression cassette driven by the maize *ubiquitin* promoter to generate the

https://doi.org/10.1038/s41467-025-64048-z

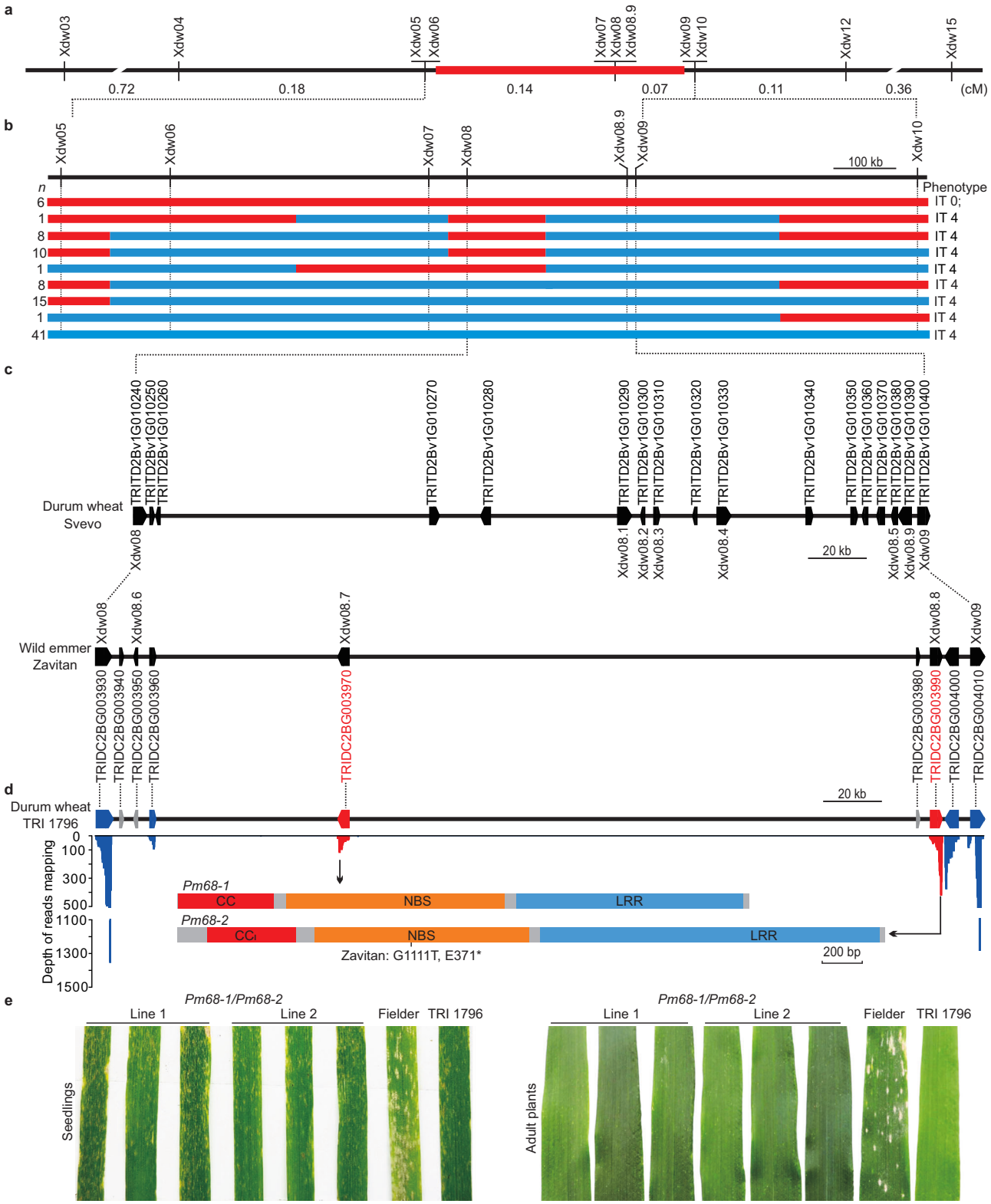

constructs pLGY02-*ZmUbi::Pm68-1* and pLGY02-*ZmUbi::Pm68-2*. These constructs were separately transformed into wheat cv. Fielder using the *Agrobacterium tumefaciens*-mediated transformation method. We obtained five independent transgenic T_0 events carrying *Pm68-1* and *Pm68-2* each. RT-PCR and qRT-PCR analyses verified the expression of the *Pm68-1* and *Pm68-2* in transgenic T_0 plants (Supplementary Fig. 5; Supplementary Fig. 6). However, all these transgenic T_0 and T_1 lines were susceptible to BgtYZ01 at both seedling and adult-plant stages (Supplementary Fig. 7). We then pyramided *Pm68-1* and *Pm68-2* transgenes by crossing the T_1 plants carrying *Pm68-1* or *Pm68-2*. The two independent F_1 plants and their selfed progenies carrying both *Pm68-1* and *Pm68-2* showed resistance to BgtYZ01 at both the seedling and adult plant stages (Fig. 1e; Supplementary Fig. 8). Trypan blue staining revealed that *Bgt*-induced cell death first observed in transgenic *Pm68-1/Pm68-2* Line 1 and TRI 1796 plants at 12 h post-inoculation (hpi), became more pronounced at 24 hpi and 48 hpi,

Fig. 1 | Map-based cloning and functional validation of *Pm68*. **a** Genetic map of the region harboring *Pm68* on the short arm of Durum wheat chromosome 2B. *Pm68* was mapped to a 0.21 cM region flanked by markers *Xdw05*/*Xdw06* and *Xdw09*/*Xdw10*. **b** Association mapping delimited *Pm68* to 266-kb and 297-kb regions corresponding to Svevo and Zavitan reference genomes, respectively. Marker analysis of the 91 durum wheat accessions grouped them into nine different haplotypes, "n" indicates the number of accessions of each haplotype. Powdery mildew infection was evaluated using a 0–4 scale. 0; and 4 represent necrotic flecks and highly susceptible (no necrosis with full sporulation) reactions, respectively. Scale bar = 100 kb. **c** Comparation of *Pm68* intervals from Svevo, Zavitan and TRI 1796 suggests the *Pm68* interval of TRI 1716 is highly similar to Zavitan and diverged from Svevo. Synteny of genes from different accessions is indicated by dot lines. Scale bar = 20 kb. **d** Read-mapping depth of the *Pm68* interval. RNA-seq data from BgtYZ01-infected leaf tissues of TRI 1796 were mapped to PacBio assembly of TRI 1796. Reads mapping data of the 305-kb *Pm68* interval were extracted and then visualized by R package ggplot2. Expressed genes are indicated by blue and red colors. Two NLR genes are highlighted in red and their gene structures are represented as rectangular bars. Predicted protein domains are differentiated by color coding. CC, coiled-coil; NBS, nucleotide-binding site; LRR, leucine-rich repeat. Scale bar = 200 bp. **e** Responses of two independent F_4 plants from crosses of different *Pm68-1* and *Pm68-2* T_1 transgenic plants to *Bgt* isolate BgtYZ01 at the seedling and adult plant stages. The experiment was repeated three times with same results.

whereas no cell death was not detected in transgenic lines expressing single NLR genes (Supplementary Fig. 9). Transgenic *Pm68-1/Pm68-2* Line 1 and TRI 1796 exhibited resistance to eight *Bgt* isolates collected from eight different regions across five provinces in China (Supplementary Fig. 10). It is concluded that *Pm68* resistance is controlled by the NLR pair *Pm68-1* and *Pm68-2*.

Pm68-2 or its N-terminal CC-like (CC_l) domain positively regulate Pm68-1 in triggering cell death

Based on the prediction of NCBI Conserved Domain Search, *Pm68-1* encodes a typical NLR with an N-terminal CC domain, a central NBS domain and a C-terminal LRR domain, while *Pm68-2* encodes a NLR without CC domain. We predicted the three-dimensional structure of the two NLRs using AlphaFold 3. Pm68-2 were predicted to have a four-helix bundle that is similar to a typical CC domain, hereby designated CC-like (CC_l) domain (Fig. 2a, b).

Functional characterization of NLR pairs is frequently performed using transient expression in *N. benthamiana*[41,42]. Therefore, we performed a series of *A. tumefaciens*-mediated transient overexpression assays of Pm68-1 and Pm68-2 in *N. benthamiana* leaves (Fig. 2c). We observed that the individual expression of Pm68-1 or Pm68-2 did not induce cell death in *N. benthamiana* leaves at 72 h post-infiltration. However, co-expression of the two full-length proteins triggered cell death response. Meanwhile, the mutant Pm68-1_{D505V}, which contains an MHD motif substitution known to cause autoactivation[43], also led to significant cell death, whereas the mutant Pm68-2_{D545V} did not exhibit this phenotype (Fig. 2d; Supplementary Fig. 11). Further analysis involved the introduction of the K210R mutation, known to impair ATP binding[44], into Pm68-1_{D505V} and Pm68-1. The mutant Pm68-$1_{K210R/D505V}$ was found to lost the ability to induce cell death compared with the autoactivation mutant Pm68-1_{D505V}, suggesting that the K210R mutation in Pm68-1 resulted in a loss of function. As expected, the expression of Pm68-1_{K210R} alone or the co-expression of Pm68-1_{K210R} and Pm68-2 did not trigger cell death. In contrast, co-expression of Pm68-1 with the mutant Pm68-2_{K255R}, where K255R corresponds to the K210R in Pm68-1, still resulted in observable cell death (Fig. 2d; Supplementary Fig. 11). Co-immunoprecipitation (Co-IP) assays revealed that Pm68-1 physically interacts with Pm68-2 and each of its three individual domains. (Supplementary Fig. 12). These findings indicate that Pm68-1 is a pivotal player in the initiation of cell death and that its activity can be regulated by Pm68-2.

To identify the domain of Pm68-2 responsible for regulating the cell death-inducing activity of Pm68-1, we co-expressed Pm68-1 or Pm68-2_CC_l with the different truncated fragments of Pm68-2 or Pm68-1 separately in *N. benthamiana* leaves. Individual expression of truncated fragments of Pm68-1 or Pm68-2, and CC domain of Pm21 were used as controls. The results revealed that only the combination of Pm68-1 and Pm68-2_CC_l induced cell death (Fig. 2d; Supplementary Fig. 11). This suggests that the CC_l domain of Pm68-2 is necessary for modulating the activity of Pm68-1.

The *Pm68* locus can be traced back to a specific wild emmer subpopulation

Comparative *k*-mer analysis revealed that TRI 1796 carries a ~1.6 Mb haplotype block that is highly diverged from the durum reference cultivar Svevo[39] and more similar to the reference assembly of wild emmer line Zavitan[40] (Supplementary Fig. 13). Identity-by-state (IBSpy) analyses[45] confirmed that the *Pm68*-containing haplotype block originated from the genetically distinct and geographically restricted judaicum wild emmer subpopulation[46], to which Zavitan belongs[47] (Supplementary Fig. 14; Supplementary Data 5).

Then we use the dominant marker *Xdw08.8*, corresponding to *Pm68-2*, to screen 120 durum wheat accessions and 118 wild emmer accessions (including Zavitan) (Supplementary Data 3). A total of 32 accessions, including 6 durum wheat and 26 wild emmer accessions, were positive for marker *Xdw08.8*. We amplified and Sanger sequenced the two NLR genes from these 32 accessions, which revealed nine *Pm68* haplotypes (Haplotypes A to I), consisting of six *Pm68-1* alleles (Supplementary Data 6) and six *Pm68-2* alleles (Supplementary Data 7). We co-infiltrated different *Pm68* allelic NLR pairs representing Haplotypes A to I into *N. benthamiana*, all of which induced cell death (Supplementary Fig. 15). All six durum wheat accessions (TRI 1796, TRI 1876, TRI 10092, PI 70716, DR64, and DR343) have the identical NLR pair (*Pm68-1/Pm68-2*), designated Haplotype A. Haplotype F (*Pm68-1*^{IW21}/*Pm68-2* ^{IW21}), found in two wild emmer accessions (IW21 and IW29), is identical to the powdery mildew resistance gene *MlIW39* reported in the companion study[48]. Compared with Haplotype A, Haplotype F/*MlIW39* only has one nucleotide variation G2324A in *Pm68-1* and one nucleotide variation T1604C in *Pm68-2* leading to amino acid substitutions R775H and M535T, respectively. The nonfunctional Haplotype C (*Pm68-1/Pm68-2*^{Zavitan}) exists in four BgtYZ01-susceptible wild emmer accessions including Zavitan, and it differs for one nucleotide (G1111T of *Pm68-2*) from Haplotype A, leading to a premature stop codon of *Pm68-2* (Fig. 1d). Another six haplotypes (Haplotypes B, D, E, G, H and I) were detected only in wild emmer accessions that showed immunity to BgtYZ01 (Supplementary Data 8; Supplementary Fig. 16), suggesting additional gene resources for the wheat powdery mildew resistance breeding.

Pm68 shows potential to be used for powdery mildew-resistance breeding in wheat

To expand the utilization of *Pm68*, we crossed *Pm68* into Chinese elite cultivar YM158, and generated two independent BC_3F_5 introgression lines. The two lines showed resistance to *Bgt* isolate BgtYZ01 at both the seedling and adult-plant stages (Fig. 3a). We evaluated their major agronomic traits and compared with the recurrent parent YM158. The traits including plant height, spike number per plant, grain number per spike, and 1000-grain weight of the introgression lines were significantly higher than those of the recurrent parent YM158 ($P < 0.05$), whereas spike length and spikelet number per spike exhibited no obvious difference between the introgression lines and YM158 (Fig. 3b–d). We also investigated the agronomic performance for the

https://doi.org/10.1038/s41467-025-64048-z

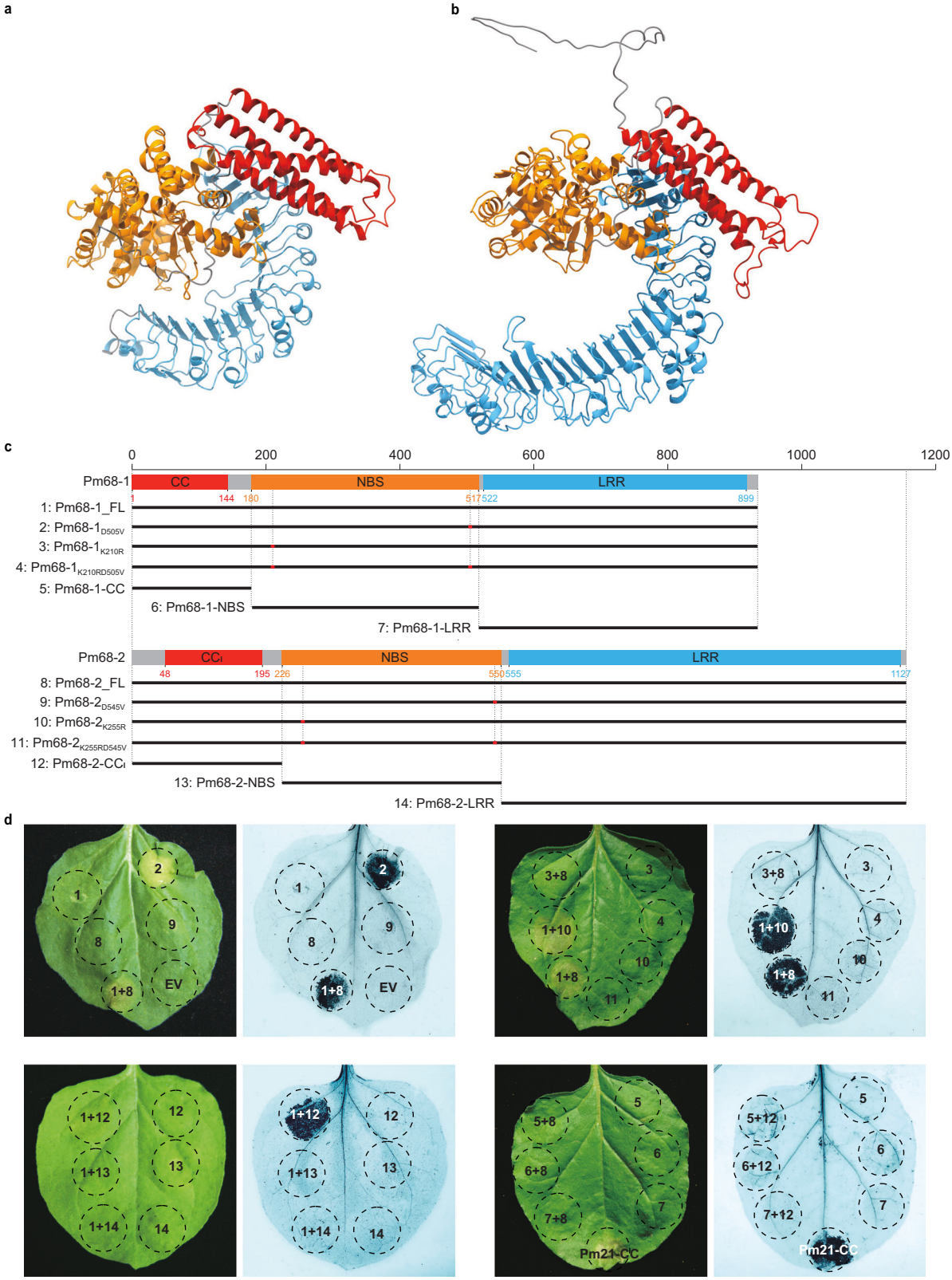

Fig. 2 | Pm68-2 or its N-terminal CC-like (CC_I) domain positively regulate Pm68-1 -mediated cell death in *Nicotiana benthamiana*. **a**, **b** Three-dimensional models of Pm68-1 and Pm68-2 predicted by AlphaFold 3. Red: CC or CC-like (CC_I) domain, orange: NBS domain, blue: LRR domain. **c** Schematic representation of constructs containing the corresponded Pm68-1 and Pm68-2 expression cassettes. **d** Cell death in *N. benthamiana* leaves at 72 h after infiltration with *Agrobacterium tumefaciens* carrying constructs of constitutive mannopine synthase (MAS) promoter-driven Pm68-1 and Pm68-2 fragments 1 to 14 illuminated above, the CC domain of Pm21 was used as a positive control. The experiment was repeated three times with similar results.

https://doi.org/10.1038/s41467-025-64048-z

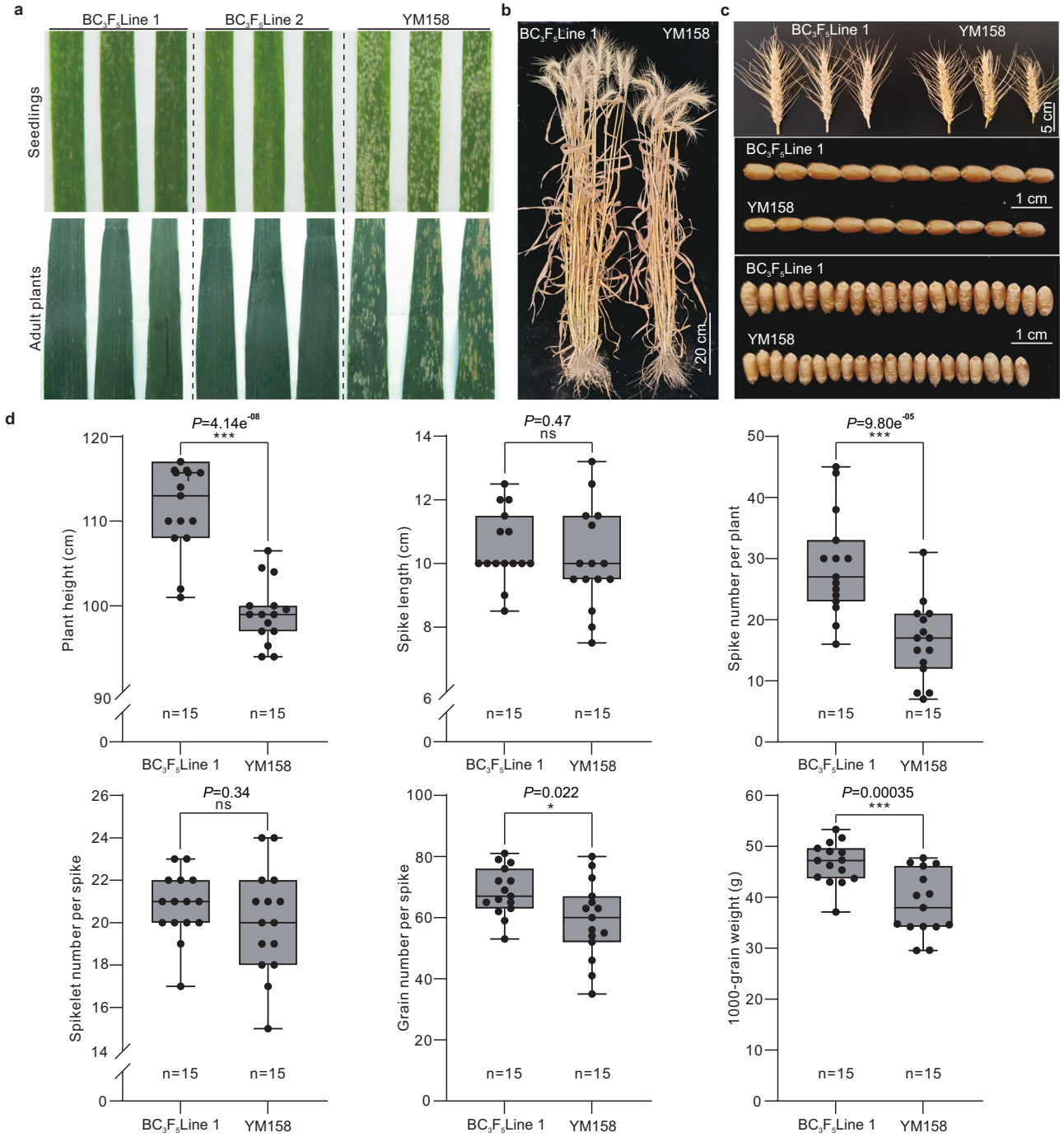

Fig. 3 | *Pm68* introgression shows no deleterious linkage drag. a The *Pm68* conferred partial resistance (IT1) and immunity (IT0) to BgtYZ01 at the seedling and adult plant stages, respectively. **b**, **c** Visual phenotypes of *Pm68* introgression line and the recurrent parent YM158 under field condition. **d** Comparing the agronomic traits between the *Pm68* introgression line and recurrent parent YM158 in plant height, spike length, spike number, spikelet number per spike, grain number per spike and 1000-grain weight under field condition. The data are displayed as box and whisker plots with individual data points. The error bars represent the maximum and minimum values. Center line, median; box limits, 25th and 75th percentiles. *P* values were calculated with a two-tailed Student's *t*-test, ns = not significant ($P > 0.05$), *$P < 0.05$, ***$P < 0.001$. The experiment was performed once with 15 biological replicates. Source data are provided as a Source Data file.

T_4 homozygous transgenic line carrying both *Pm68-1* and *Pm68-2*. All the tested agronomic traits showed no significant difference between the *Pm68* transgenic lines and the untransformed Fielder (Supplementary Fig. 17). In addition, the overexpression of *Pm68-1*/*Pm68-2* in transgenic wheat lines did not cause visible hypersensitive response (HR) or spontaneous necrosis in leaves (Supplementary Fig. 18). These results suggest that *Pm68* introgression is not associated with deleterious linkage drag and *Pm68* has no obvious negative effects on the major agronomic traits, which highlights the potential value of *Pm68* in powdery mildew resistance breeding of wheat.

Discussion

Pm68 was mapped to the terminal part of 2BS in Greek durum wheat accession TRI 1796[38]. In this study, we adopted an integrated approach, involving genetic fine mapping using a biparental population, association analysis of durum wheat natural population, and PacBio

sequencing and assembling of TRI 1796 genome, to isolate *Pm68*. Stable transgenic complementation assays revealed that *Pm68* resistance is mediated by a pair of NLR genes, *Pm68-1*/*Pm68-2*. Biparental population based fine-mapping and natural population-based association mapping delimited *Pm68* to 266-kb or 297-kb intervals correspond to different reference genomes. Low-coverage (~10 x) PacBio genome sequencing of resistance donor accession provided reference for candidate gene mining, and RNA-seq reads mapping helped to reduce the number of candidate genes. As sequencing costs are continuously decreasing, the integrated approach could accelerate gene cloning in plant species with large genome, such as wheat.

In plants, NLR proteins belong to the major class of immune receptors that recognize pathogen effectors and activate effector-triggered immunity (ETI)[49]. Plant NLRs likely evolved from singleton NLRs to NLR pairs and then to NLR networks[50]. Singleton NLRs can both recognize effectors directly or indirectly and activate cell death and defence responses, such as the wheat stem rust resistance protein Sr35[51] and *Arabidopsis Pseudomonas syringae* resistance protein ZAR1[52,53]. Some NLRs function in genetically linked pairs, which consist of a sensor NLR and a helper/executor NLR that are specialized to recognize the pathogen and initiate immune signaling, respectively. For examples, the rice (*Oryza sativa* L.) NLR pairs RGA4/RGA5[41] and Pikp1/Pikp2[54] confer resistance to *Magnaporthe oryzae*. Transient overexpression of the helper/executor NLR RGA4 could induce cell death in *N. benthamiana* leaves, which can be inhibited by the co-expressed sensor NLR RGA5, through forming a hetero-complex. Co-expression of RGA4, RGA5, and the corresponding effector AVR-Pia also triggered cell death[55]. In the Pikp-1/Pikp-2 pair, neither co-expression of them or expression of them alone trigger cell death, while co-expression of Pikp-1, Pikp-2, and the corresponding effector AVR-PikD induced cell death, suggesting that the Pikp-1/Pikp-2 complex needs to be activated by AVR-PikD[44]. Unlike previous reported NLR pairs, transient co-expression of *Pm68-1* and *Pm68-2* triggered cell death in *N. benthamiana* leaves, while expression of either single NLR did not induce cell death, and co-expression of *Pm68-1* and N-terminal CC_I domain of *Pm68-2* also induced cell death, suggesting a different activation mechanism of this NLR pair.

Our results also showed that an autoactivation variant of Pm68-1, rather than Pm68-2, induced cell death in *N. benthamiana* leaves, indicating only Pm68-1 is capable of inducing cell death upon the activated state. In addition, co-expression of the loss-of-function mutant Pm68-1_{K210R} with Pm68-2 did not induce cell. This observation indicates that the Pm68-1 functions as a helper/executor NLR in *Pm68-1*/Pm68-2-mediated cell death. Pm68-2 could be a sensor NLR that directly or indirectly recognizes effectors from avirulent *Bgt* pathogens. Haplotype analysis reveals greater diversification in *Pm68-2* alleles than in *Pm68-1* alleles, consistent with sensor NLR divergence versus helper/executor NLR conservation (Supplementary Data 6 and 7). Pm68-2 is an atypical NLR that its CC_I domain shows no sequence homology, but structural resemblance to typical CC domains of NLRs. Expression of Pm68- 2 or its CC_I domain activated Pm68-1 and triggered cell death in *N. benthamiana* leaves. Therefore, the CC_I domain of Pm68-2 is essential for modulating the activity of Pm68-1. We suppose that the CC_I domain serve as a regulatory interface, facilitating the interactions between Pm68-1 and Pm68-2 and controlling the activation of cell death response. Unlike the heterologous expression system, transgenic plants carrying both maize *ubiquitin* promoter-driven *Pm68-1* and *Pm68-2* exhibited no autoimmunity or spontaneous necrosis while gaining resistance to powdery mildew (Supplementary Fig. 18). Trypan blue staining showed sporadic cell death at *Bgt* infection sites in TRI 1796 and transgenic *Pm68-1/Pm68-2* Line 1, whereas no cell death occurred in transgenic lines expressing single NLR genes (Supplementary Fig. 9). The above results indicate that the Pm68-1/Pm68-2 complex is constitutively active in heterologous systems but maintains an inactive and primed state in homologous systems. This suggests that a regulatory component absent from heterologous systems might be required for suppression of auto-activation. Our findings provide insights into the molecular mechanism underlying the regulation of activity by this unique pair of NLRs[48].

Distant hybridization has played a significant role in the improvement and breeding of wheat, which has greatly enriched wheat genetic diversity. For example, more than 40% of the disease resistance genes used in common wheat breeding are introgressed from outside the common wheat gene pool[5]. However, recombination suppression resulted linkage drag has become a major obstacle that restricts the wide application of this strategy. Wild emmer, which is considered a progenitor of cultivated tetraploid and hexaploid wheat, and durum wheat shared the same sets of A and B genome with common wheat[56]. Therefore, relatively mild or no recombination suppression allows gene introgression without linkage drag. Considering the effectiveness of *Pm68* against all the 22 *Bgt* isolates tested[38], we transferred *Pm68* from durum wheat TRI 1796 into the elite common wheat cultivar YM158 through interspecific cross and multiple backcrosses and self-crosses. When challenged by *Bgt* isolate BgtYZ01, the introgression lines carrying *Pm68* showed effective resistance (scored IT 1) at the seedling stage and immunity at the adult plant stage (Fig. 3a). The introgression lines did not show any obviously adverse effects on the major agronomic traits, except for a slight increase of plant height, which may be inherited from TRI 1796 (~152 cm). Conversely, the introgression lines exhibited superior agronomic traits, which was probably an outcome of larger biomass. We also did not observe significant differences between transgenic plants with the overexpressed *Pm68-1/Pm68-2* pair and the untransformed control Fielder. The above results highlight the disease-resistance breeding value of *Pm68* in both durum wheat and common wheat.

Methods

Plant materials and growth conditions

A panel of 120 durum wheat accessions was ordered from the Genebank Information System of the IPK Gatersleben (GBIS-IPK), the U.S. National Plant Germplasm System (NPGS), and the Chinese Crop Germplasm Resources Information System (CCGRIS) (Supplementary Data 3). A total of 118 wild emmer accessions were ordered from the NPGS or kindly provided by Dr. Z. Y. Liu of Institute of Genetics and Developmental Biology, Chinese Academy of Sciences, Beijing, China and Dr. H. Li of Henan University, Kaifeng, China (Supplementary Data 3). The resistant durum wheat accession TRI 1796, carrying *Pm68*[38], was crossed with the susceptible accession PI 584832, and the derived 1382 F_2 individuals were used for genetic mapping of *Pm68*. The susceptible wheat cultivar Yangmai 23 (YM23) was used for reproducing *Bgt* conidiospores to prepare inoculum. The susceptible wheat cultivar Fielder was used as the recipient for transformation. The susceptible wheat cultivar Yangmai 158 (YM158) was used as the recurrent parent when transferring *Pm68* from durum wheat TRI 1796 into common wheat. *N. benthamiana* was used for transient expression assays. All plants were grown in a greenhouse with LED lighting under long-day conditions (16 h light/8 h dark) at 24 °C.

Evaluation of powdery mildew resistance

A total of 1382 F_2 plants and 20 plants of each F_3 family that exhibited recombination events at the one-leaf stage were inoculated with the *Bgt* isolate BgtYZ01, which was collected in Yangzhou, China[57], by dusting fungal conidiospores from YM23 leaves. Responses to powdery mildew were evaluated 8–10 days post-inoculation (dpi) according to the infection types (IT) scored on a scale from 0 to 4, where ITs 0, 0, 1, and 2 were classified as resistant, and ITs 3 and 4 as susceptible[58]. Powdery mildew IT values of ten plants of each durum wheat accession and the *Xdw08.9*-positive wild emmer were also tested.

The resistance spectrum of transgenic *Pm68-1/Pm68-2* Line 1 and durum wheat TRI 1796 were was examined in seedling tests with three replicates using BgtYZ01 and the other seven *Bgt* isolates collected from different regions of China by Dr. Yinghui Li (Triticeae Research Institut, Sichuan Agricultural University, Chengdu, China). Common wheat Fielder and durum wheat PI 584832 were used as the controls. Leaves were cut into segments ~3 cm in length and placed in Petri dishes containing 8.0 g/L agar and 50 mg/L benzimidazole. Leaves on Petri dishes were inoculated with the above eight *Bgt* isolates separately and maintained ex vivo at 22 °C on 16 h light/8 h dark cycle[59]. Pictures of powdery mildew responses were taken at 8 days post inoculation.

Development of and application of molecular markers for genotyping

Ten co-dominant markers (*Xdw03* – *Xdw10*, *Xdw12* and *Xdw15*) were reported in our previous work[38] and one co-dominant markers (*Xdw08.9*) were developed in this study according to the surrounding sequences of the InDel regions between durum wheat cultivars Svevo[39] (https://www.interomics.eu/durum-wheat-genome) and Kronos (https://opendata.earlham.ac.uk/opendata/data/Triticum_turgidum/EI/v1.1). In addition, five PI 584832-dominant markers (*Xdw08.1* – *Xdw08.5*) and three TRI 1796-dominant markers (*Xdw08.6* – *Xdw08.8*) were designed based on the differential genes between the reference genomes of durum wheat cultivar Svevo and wild emmer accession Zavitan[40]. The primers of all polymorphic markers can be found in Supplementary Data 1.

Genomic DNA used for genotyping was extracted from seedling leaves using the CTAB method. PCR amplification was carried out in a T100 thermal cycler (Bio-Rad, Hercules, CA, USA) using an initial denaturation at 94 °C for 3 min, 35 cycles of 10 s at 94 °C, 30 s at 60 °C, 1 min at 72 °C, and a final extension for 5 min at 72 °C. Twenty-five microlitres of reaction mixture contained 1× PCR buffer, 0.2 mM of each dNTP, 2 µM of each primer, 50 ng genomic DNA, and 1 Unit of Taq DNA polymerase (TaKaRa, Shiga, Japan, Catalog No. R001A). PCR products were separated in 8% non-denaturing polyacrylamide gels, followed by silver staining, or separated in 1.2% agarose gel stained with GelRed.

Fine genetic mapping of *Pm68*

A total of 1382 F_2 individuals derived from the cross between TRI 1796 and PI 584832 were used to map *Pm68*. The flanking markers *Xdw03* and *Xdw15* were initially used for screening recombination events in the above mapping population. Then, 41 individuals containing recombination events were phenotyped at the one-leaf stage with *Bgt* isolate BgtYZ01 and genotyped by a set of markers described above (Supplementary Data 1 and 2). Finally, 41 F_3 families were generated from the F_2 individuals containing recombination events, and 20 plants of each F_3 family at the one-leaf stage were phenotyped again using BgtYZ01.

Marker analysis of different durum wheat accessions

To further narrow the *Pm68* locus, 85 susceptible and 6 resistant durum wheat accessions were genotyped with 15 markers, including seven co-dominant markers, five PI 584832-dominant markers (*Xdw08.1* – *Xdw08.5*) and three TRI 1796-dominant markers (*Xdw08.6* – *Xdw08.8*) (Supplementary Data 1 and 4).

PacBio HiFi sequencing and assembling of TRI 1796 genome

PacBio HiFi sequencing was conducted by BGI (Shenzhen, China). High molecular weight genomic DNA was extracted from TRI 1796 seedling leaves using the CTAB method and then sheared to 15–20 kb using Diagenode Megaruptor system (Diagenode, Seraing, Belgium). PacBio HiFi sequencing library was constructed using SMRTbell Express Template Prep Kit 2.0 and DNA fragment size was selected with the BluePippin System (Sage Science, Beverly, MA, USA). High-throughput sequencing was conducted on PacBio Sequel IIe system (Pacific Biosciences, Menlo Park, CA, USA). The PacBio HiFi reads were assembled using hifiasm (v.0.19.8) with default parameters and then evaluated using seqkit (v.2.6.1)[60,61].

Transcriptome sequencing of TRI 1796 leaves and read-mapping analysis

The seedling of TRI 1716 was inoculated with *Bgt* isolate BgtYZ01 and the leaf sample was collected at 24 h post inoculation. Total RNA was extracted using Illumina TruSeq RNA Sample Prep Kit (Illumina, Inc., San Diego, CA, USA), and then used for RNA sequencing on the Illumina NovaSeq 6000 platform. The low quality reads and adapter contaminations were removed with Trimmomatic v0.40[62]. Subsequently, the high quality reads were aligned to the TRI 1716 genome assembly using STAR (2.7.11b) with default parameters. The BAM file corresponding to the 305-kb *Pm68* interval flanked by markers *Xdw08* and *Xdw09* in contig ptg004078l was extracted using Geneious Prime (v.2020.2.4). Then, the average read coverage depth per 100 bp for the 305-kb interval was calculated using samtools (v.1.19.2) and then visualized by R package ggplot2 (v.3.5.0).

K-mer analysis

The 51-mers datasets were generated from the durum wheat Svevo and wild emmer wheat Zavitan genomes using kmc (3.2.4), respectively, and then mapped to the TIR 1796 assembly using bwa (0.7.17), with only perfect alignments outputted (-T 51). Non-overlapping bins of length 100 bp were created using bedtools (2.31.0), and the *k*-mer mapping coverage within each bin was calculated using samtools (1.19.2). For visualization, the R package ggplot2 (v.3.5.0) was employed to plot the mapping coverage distribution of *k*-mers from Svevo and Zavitan, and the distribution of the mapping coverage differences of *k*-mers from Svevo and Zavitan.

Identity-by-state (IBSpy) analyses

The 68 publicly available wild emmer whole genome sequences[63–66] and the reference genome Zavitan[40] (Supplementary Data 5) were downloaded and the whole genome sequencing (WGS) raw data were trimmed with Trimmomatic (v. 0.39) with the following settings: LEADING:3 TRAILING:3 SLIDINGWINDOW:4:25 MINLEN:75. From the trimmed WGS sequences and the Zavitan reference genome, all the canonical 31-mers were counted using kmc (v 3.1.2). We compared the 69 wild emmer accession to the contig ptg004078l containing the *Pm68* from the TRI 1796 assembly using IBSpy (v0.4.6) in 50 kb windows. We also run IBSpy with the Zavitan genome assembly as reference with the same settings to identify the judaicum accessions present in the panel.

Protein domain and three-dimensional model prediction

Domains of Pm68-1 and Pm68-2 were predicted using NCBI Conserved Domain Search (https://www.ncbi.nlm.nih.gov/Structure/cdd/wrpsb.cgi). Three-dimensional models of Pm68-1 and Pm68-2 were predicted by AlphaFold 3[67].

RT-PCR and quantitative real-time RT-PCR (qRT-PCR) analysis

The seedlings of durum wheat cultivar TRI 1796 were inoculated with *Bgt* isolate BgtYZ01 as described above. Leaf samples were collected at 0, 12 and 24 h post-inoculation (hpi) for extracting total RNA with the RNAiso Plus Kit (TaKaRa, Shiga, Japan, Catalog No. 9109). Two micrograms of total RNA were then used to synthesize the first-strand cDNA with the PrimeScript™ II 1st Strand cDNA Synthesis Kit (TaKaRa, Shiga, Japan, Catalog No. 6210 A). The candidate genes *Pm68-1* and *Pm68-2* were PCR amplified from cDNAs (0 hpi) using the high fidelity PrimeSTAR Max Premix (TaKaRa, Shiga, Japan, Catalog No. R045A) with primer pairs P1/P2 and P3/P4, followed by Sanger sequencing with

primers P5 to P8 and P9 to P13, respectively. qRT-PCR was performed using TB Green Premix Ex Taq™ II (TaKaRa, Shiga, Japan, Catalog No. RR820A) in Applied Biosystems QuantStudio 3 Real-Time PCR System (Thermo Fisher Scientific, Waltham, USA) with primer pairs P14/P15 and P16/P17 for *Pm68-1* and *Pm68-2*, respectively. The gene *actin* was used as the internal control. The $2^{-\Delta\Delta Ct}$ method[68] was used to evaluate relative transcription levels of transgenes.

Plasmid construction and wheat transformation

The coding sequences of *Pm68-1* and *Pm68-2* were amplified from genomic DNA of TRI 1796 using the high fidelity PrimeSTAR Max Premix (TaKaRa, Shiga, Japan, Catalog No. R045A) and primer pairs P1/P2 and P3/P4, respectively (Supplementary Data 9). The PCR products of the two genes were cut with *Sma*I and *Spe*I and ligated into the downstream of maize *ubiquitin* promoter in the binary vector pLGY02[13] to generate pLGY02-*ZmUbi::Pm68-1* and pLGY02-*ZmUbi::Pm68-2*, respectively. After confirming by Sanger sequencing using primers P5 – P8 for *Pm68-1* and primers P9 – P13 for *Pm68-2* (Supplementary Data 9), the two constructs were separately transformed into the susceptible wheat cultivar Fielder by the *Agrobacterium tumefaciens*-mediated transformation method[69].

Transgenic assays

The T_0 plants of *Pm68-1* and *Pm68-2* were detected for the presence and absence of the transgene by PCR using primer pairs P8/P20 and P13/P20, respectively. Total RNA was extracted from T_0 leaves for the synthesis of the first-strand cDNA with the PrimeScript™ II 1st Strand cDNA Synthesis Kit (TaKaRa, Shiga, Japan, Catalog No. 6210 A). qRT-PCR was performed with primer pairs P14/P15 and P16/P17 for *Pm68-1* and *Pm68-2*, respectively (Supplementary Data 9). Wheat gene *actin* was used as the internal control. The $2^{-\Delta\Delta Ct}$ method[68] was used to evaluate relative transcription levels of transgenes. Ten transgene-positive plants in each T_1 families of *Pm68-1* and *Pm68-2* at the seedling and the adult-plant stages were successively inoculated with *Bgt* isolate BgtYZ01 to test their responses to powdery mildew. The *Pm68-1*-positive T_1 lines 1 and 2 were crossed with the *Pm68-2*-positive T_1 lines 1 and 2, respectively. The generated F_1 to F_4 plants were detected with primer pairs P8/P20 for *Pm68-1* and P13/P20 for *Pm68-2*, respectively. Finally, the F_4 families of the two crosses pyramiding the pair of *Pm68-1* and *Pm68-2* were obtained. Ten plants of each F_4 family derived the two crosses were inoculated with *Bgt* isolate BgtYZ01 at the seedling and the adult-plant stages to assess their powdery mildew responses.

Histochemical detection of cell death in transgenic wheat and durum wheat leaves

Transgenic lines with single *Pm68-1*, single *Pm68-2* and pair *Pm68-1*/*Pm68-2* and durum wheat TRI 1796 were inoculated with *Bgt* isolate BgtYZ01 at the one-leaf stage. At 0, 12 24 and 48 hpi, leaves were cut and immersed in a trypan blue staining solution (2.5 mg/ml trypan blue, 25% lactic acid, and 23% saturated phenol) for 30 min in boiling wate, destained with Chloral hydrate solution (2.5 g/ml) for 3 d and stained with 0.6% Comassie brilliant blue R-250 solution for 10 s. Images were taken using a Leica DM2500 microscope.

Cell death assays on *N. benthamiana*

The CDS of *Pm68-1* and *Pm68-2*, along with their respective domain-encoding sequences, were amplified from TRI 1796 using high fidelity PrimeSTAR GXL DNA polymerase (TaKaRa, Shiga, Japan, Catalog No. R050A). The CDSs without stop codons were cloned into the pS1300-Flag-Nos vector (C-terminally fused with Flag) with an expression cassette driven by the constitutive mannopine synthase (MAS) promoter utilizing the ClonExpress Ultra One Step Cloning Kit (Vazyme, Nanjing, China; Catalog No. C115-01). Individual domain-encoding fragments were cloned into either the pS1300-Flag-Nos or pS1300-GFP-Nos vectors to obtain C-terminally Flag- or GFP-tagged fusions. Fragments containing the P-loop mutations (K210R for Pm68-1 and K255R for Pm68-2) and/or the autoactive mutations (D505V for Pm68-1, D545V for Pm68-2) were generated using the overlap extension PCR method[70], resulting in specific amino acid substitutions at the target positions. These mutated PCR products were subsequently cloned into the pS1300-Flag-Nos vector. All constructs were confirmed by Sanger sequencing using primers listed in Supplementary Data 9. In cell death assays, the construct containing the encoding sequence of the CC domain of *Pm21* was used as the positive control[71].

The above constructs were transformed into *Agrobacterium* strain GV3101, separately. Transformed *Agrobacterium* was cultured overnight at 28 °C in Luria-Bertani broth supplemented with 50 mg/mL rifampicin and 50 mg/mL kanamycin. The bacteria were harvested by centrifugation and suspended in infiltration medium (2% sucrose, 0.5% MS basal salts, 10 mM MES, pH 5.6, and 200 µM acetosyringone) to an OD_{600} of 1. The suspension was incubated at room temperature for 1–3 h prior to infiltration into *N. benthamiana* leaves. For co-infiltration experiments, *Agrobacterium* cultures were mixed in a 1:1 ratio with either another construct or infiltration medium. The infiltrated *N. benthamiana* plants were maintained at room temperature and photographed at 48 hpi. The infiltrated leaves were stained using a trypan blue solution (10 mL lactic acid, 10 ml glycerol, 10 g phenol, 10 mg trypan blue, and 50 mL ethanol, dissolved in 30 mL distilled water) in boiling water for 5 min. Stained leaves were immersed in chloral hydrate solution (2.5 g/mL) until the background was no longer visible. *Agrobacterium* strain GV3101 harboring the empty vector was used as a negative control.

Protein extraction and Western blotting analysis

Leaf tissues for protein extraction were sampled at 24 h post-infiltration. A total of 0.1 g of frozen leaf tissues were ground to fine powder for each sample. Total proteins were extracted in 0.5 mL extraction buffer [50 mM Tris-HCl (pH7.5), 150 mM NaCl, 1 mM EDTA, 1% NP-40, 0.1% SDS, 0.25% deoxycholate, 10 mM dithiothreitol (DTT), and 1× cocktail (protease inhibitor, Roche, Basel, Switzerland, Catalog No. 4693116001)]. The lysates were centrifuged at 18,000 × *g* for 20 min at 4 °C. The supernatants were collected and incubated in 1× Laemmli buffer at 95 °C for 5 min.

The heated protein samples were then separated by 12% (w/v) sodium dodecyl sulfate-polyacrylamide gel electrophoresis (SDS-PAGE) and transferred to a PVDF membrane (Millipore, Boston, MA, USA; Catalog No. IPVH08100). Immunoblots were probed with either anti-Flag (Proteintech, Wuhan, China; Catalog No. 66008-4-lg), anti-GFP (Proteintech, Wuhan, China; Catalog No. 66002-2-lg) or anti-HA (Proteintech, Wuhan, China; No. 51064-2-AP) antibodies diluted to 1:5000. The secondary antibody, HRP-conjugated Affinipure Goat Anti-Mouse IgG (Proteintech, Wuhan, China; Catalog No. SA00001-1), was applied at a dilution of 1:5000 to detect the primary antibody. Blots were visualized using SuperSignal maximum sensitivity substrate (Proteintech, Wuhan, China, Catalog No. PK10002) and a ChemiDog imaging system (Tanon, Shanghai, China). Ponceau staining was employed to ensure equal loading across protein samples.

Co-immunoprecipitation (Co-IP) assays

The CDS of *Pm68-1* was cloned into pS1300-HA-Nos (C-terminal HA fusion) vector via homologous recombination described above. After Sanger sequencing verification, the resulting construct was transformed into *Agrobacterium* strain GV3101. Other constructs used for Co-IP assays have been described in the method section of cell death assays. Equal volumes (1:1, v/v) of *Agrobacterium* cultures harboring the *Pm68-1-HA* and the *Pm68-2-Flag*, *Pm68-1-Flag* and *Pm68-2-CC$_I$-GFP*, *Pm68-1-Flag* and *Pm68-2-NBS-GFP*, *Pm68-1-Flag* and *Pm68-2-LRR-GFP*, *Pm68-1-Flag* and *GFP* constructs were mixed and co-infiltrated into *N. benthamiana* leaves, respectively. To avoid cell death induced by overexpression of *Pm68-1* and *Pm68-2*, *Agrobacteria*-infiltrated *N.*

benthamiana tissue was collected at 24 h post infiltration. Total protein was extracted from 0.2 g of infiltrated leaf tissue using 1 mL of extraction buffer containing 50 mM Tris-HCl (pH 7.5), 150 mM NaCl, 1 mM EDTA, 1% NP-40, 0.1% SDS, 0.25% sodium deoxycholate, 10 mM dithiothreitol (DTT), and 1× protease inhibitor cocktail (Roche). Following centrifugation at 20,000 × *g* for 15 min at 4 °C, the supernatant was incubated with 10 µL of pre-washed anti-Flag magnetic beads (Yeasen, Catalog No. 20765ES40) under constant rotation overnight at 4 °C. Beads were collected using a magnetic stand (DynaMag™-2, Thermo Fisher Scientific) and washed three times with TBS buffer. Bound proteins were eluted with 50 µL of 1× Laemmli buffer by boiling at 95 °C for 5 min. Proteins from crude extracts (input) and immunoprecipitated proteins were analyzed by immunoblotting as described above.

Sanger sequencing of *Pm68-1* and *Pm68-2* isolated from durum wheat and wild emmer

The genomic DNAs of the collection of 118 wild emmer accessions were first genotyped with the dominant marker *Xdw08.8*, corresponding to *Pm68-2*. The genomic DNAs of 20 positive wild emmer and 6 positive durum wheat accessions found above were used as templates for PCR cloning of *Pm68-1* and *Pm68-2*. PCR amplifications were performed using the high fidelity PrimeSTAR Max DNA polymerase (TaKaRa, Shiga, Japan, Catalog No. R045A) with primer pairs P1/P2 and P3/P4 followed by Sanger sequencing using primers P5–P8 and P9–P13 for *Pm68-1* and *Pm68-2*, respectively.

Development of wheat introgression lines carrying *Pm68*

To transfer *Pm68* from durum wheat into wheat, crosses were carried out using the elite wheat cultivar YM158 and TRI 1796 as the female and male parents, respectively. The progenies were then backcrossed with YM158 three times, followed five generations of selfing in greenhouse conditions. In each generation, the co-segregating marker *Xdw08.9* was used to screen the individuals carrying *Pm68*. Finally, BC_3F_5 lines with *Pm68* introgression were obtained and tested with BgtYZ01 at the seedling and the adult-plant stages as described above.

Agronomic traits evaluation of *Pm68* introgression lines and *Pm68* transgenic lines

In growing season 2023–2024, two *Pm68* introgression lines and recurrent parent YM158, two *Pm68* transgenic lines and non-transgenic Fielder were planted in experimental fields at Songjiang, Shanghai and Jiangsu University (Zhenjiang, China), respectively, for agronomic trait evaluation. Twenty seeds of each wheat line were sown in a row designed as 1.5 m in length with 20 cm inter-row space. Each line was sown in three replicate rows. The major agronomic traits, including plant height (cm), spike length (cm), spike numbers per plant, spikelet numbers per spike, grain numbers per spike, and 1000-grain weight were determined using five plants of each row. The significance of differences among means of the above agronomic traits was analyzed using two-tailed Student's *t*-test.

Reporting summary

Further information on research design is available in the Nature Portfolio Reporting Summary linked to this article.

Data availability

The PacBio HiFi reads and Illumina RNA-Seq data of TRI 1796 carrying *Pm68* were deposited in the Sequence Read Archive (SRA) database under accession SRR31057414 and SRR31534046, respectively. The sequences of *Pm68-1* and *Pm68-2* alleles isolated from durum wheat and wild emmer wheat accessions have been deposited in GenBank under the accession numbers PQ655406–PQ655417 [https://www.ncbi.nlm.nih.gov/nuccore/PQ655417]. Source data are provided with this paper.

References

1. Li, H. et al. Wheat breeding in northern China: achievements and technical advances. *Crop J.* **7**, 718–729 (2019).
2. Cakmak, I., Pfeiffer, W. H. & McClafferty, B. Biofortification of durum wheat with zinc and iron. *Cereal Chem.* **87**, 10–20 (2010).
3. Sotiropoulos, A. G. et al. Global genomic analyses of wheat powdery mildew reveal association of pathogen spread with historical human migration and trade. *Nat. Commun.* **13**, 4315 (2022).
4. He, H. et al. A kinase fusion protein from *Aegilops longissima* confers resistance to wheat powdery mildew. *Nat. Commun.* **15**, 6512 (2024).
5. McIntosh, R. A. et al. Catalogue of gene symbols for wheat: 2017 supplement (KOMUGI Wheat Genetic Resource Database). https://shigen.nig.ac.jp/wheat/komugi/genes/symbolClassList.jsp (2017).
6. He, H. et al. Characterization of a new gene for resistance to wheat powdery mildew on chromosome 1RL of wild rye *Secale sylvestre*. *Theor. Appl. Genet.* **134**, 887–896 (2021).
7. Hewitt, T. et al. A highly differentiated region of wheat chromosome 7AL encodes a *Pm1a* immune receptor that recognizes its corresponding *AvrPm1a* effector from *Blumeria graminis*. *N. Phytol.* **229**, 2812–2826 (2021).
8. Sánchez-Martín, J. et al. Rapid gene isolation in barley and wheat by mutant chromosome sequencing. *Genome Biol.* **17**, 221 (2016).
9. Yahiaoui, N., Srichumpa, P., Dudler, R. & Keller, B. Genome analysis at different ploidy levels allows cloning of the powdery mildew resistance gene *Pm3b* from hexaploid wheat. *Plant J.* **37**, 528–538 (2004).
10. Sánchez-Martín, J. et al. Wheat *Pm4* resistance to powdery mildew is controlled by alternative splice variants encoding chimeric proteins. *Nat. Plants* **7**, 327–341 (2021).
11. Xie, J. et al. A rare single nucleotide variant in *Pm5e* confers powdery mildew resistance in common wheat. *N. Phytol.* **228**, 1011–1026 (2020).
12. Hurni, S. et al. Rye *Pm8* and wheat *Pm3* are orthologous genes and show evolutionary conservation of resistance function against powdery mildew. *Plant J.* **76**, 957–969 (2013).
13. Zhu, S. et al. Orthologous genes *Pm12* and *Pm21* from two wild relatives of wheat show evolutionary conservation but divergent powdery mildew resistance. *Plant Commun.* **4**, 100472 (2023).
14. Li, H. et al. Wheat powdery mildew resistance gene *Pm13* encodes a mixed lineage kinase domain-like protein. *Nat. Commun.* **15**, 2449 (2024).
15. Singh, S. P. et al. Evolutionary divergence of the rye *Pm17* and *Pm8* resistance genes reveals ancient diversity. *Plant Mol. Biol.* **98**, 249–260 (2018).
16. He, H. et al. *Pm21*, encoding a typical CC–NBS–LRR protein, confers broad-spectrum resistance to wheat powdery mildew disease. *Mol. Plant* **11**, 879–882 (2018).
17. Lu, P. et al. A rare gain of function mutation in a wheat tandem kinase confers resistance to powdery mildew. *Nat. Commun.* **11**, 680 (2020).
18. Zhu, K. et al. An atypical NLR pair *TdCNL1/TdCNL5* from wild emmer confers powdery mildew resistance in wheat. *Nat. Genet.* **57**, 1553–1562 (2025).
19. Li, M. et al. A membrane associated tandem kinase from wild emmer wheat confers broad-spectrum resistance to powdery mildew. *Nat. Commun.* **15**, 3124 (2024).
20. Krattinger, S. G. et al. A putative ABC transporter confers durable resistance to multiple fungal pathogens in wheat. *Science* **323**, 1360–1363 (2009).
21. Li, M. et al. A CNL protein in wild emmer wheat confers powdery mildew resistance. *N. Phytol.* **228**, 1027–1037 (2020).
22. Moore, J. W. et al. A recently evolved hexose transporter variant confers resistance to multiple pathogens in wheat. *Nat. Genet.* **47**, 1494–1498 (2015).

23. Lu, C. et al. Wheat *Pm55* alleles exhibit distinct interactions with an inhibitor to cause different powdery mildew resistance. *Nat. Commun.* **15**, 503 (2024).
24. Zhao, Y. et al. *Pm57* from *Aegilops searsii* encodes a tandem kinase protein and confers wheat powdery mildew resistance. *Nat. Commun.* **15**, 4796 (2024).
25. Zou, S., Wang, H., Li, W., Kong, Z. & Tang, D. The NB-LRR gene *Pm60* confers powdery mildew resistance in wheat. *N. Phytol.* **218**, 298–309 (2018).
26. Li, Y. et al. Dissection of a rapidly evolving wheat resistance gene cluster by long-read genome sequencing accelerated the cloning of *Pm69*. *Plant Commun.* **5**, 100646 (2024).
27. Gaurav, K. et al. Population genomic analysis of *Aegilops tauschii* identifies targets for bread wheat improvement. *Nat. Biotechnol.* **40**, 422–431 (2022).
28. Han, G. et al. Two functional CC-NBS-LRR proteins from rye chromosome 6RS confer differential age-related powdery mildew resistance to wheat. *Plant Biotechnol. J.* **22**, 66–81 (2024).
29. Ma, C. et al. An *Aegilops longissima* NLR protein with integrated CC-BED module mediates resistance to wheat powdery mildew. *Nat. Commun.* **15**, 8281 (2024).
30. He, H. et al. An integrated pipeline facilitates fast cloning of a new powdery mildew resistance gene from the wheat wild relative *Aegilops umbellulata*. *Plant Commun.* **5**, 101070 (2024).
31. Athiyannan, N., Aouini, L., Wang, Y. & Krattinger, S. G. Unconventional R proteins in the botanical tribe Triticeae. *Essays Biochem* **66**, 561–569 (2022).
32. Li, Y., Govta, L., Sung, Y., Coaker, G. & Fahima, T. The spectrum of diverse disease-resistance genes cloned and characterized in the Triticeae tribe. *Ann. Rev. Phytopathol.* **15**, 40 (2025).
33. Sánchez-Martín, J. & Keller, B. NLR immune receptors and diverse types of non-NLR proteins control race-specific resistance in Triticeae. *Curr. Opin. Plant Biol.* **62**, 102053 (2021).
34. Bennett, F. G. A. Resistance to powdery mildew in wheat: a review of its use in agriculture and breeding programmes. *Plant Pathol.* **33**, 279–300 (1984).
35. Srichumpa, P., Brunner, S., Keller, B. & Yahiaoui, N. Allelic series of four powdery mildew resistance genes at the *Pm3* locus in hexaploid bread wheat. *Plant Physiol.* **139**, 885–895 (2005).
36. Yahiaoui, N., Brunner, S. & Keller, B. Rapid generation of new powdery mildew resistance genes after wheat domestication. *Plant J.* **47**, 85–98 (2006).
37. Zhu, Z., Kong, X., Zhou, R. & Jia, J. Identification and microsatellite markers of a resistance gene to powdery mildew in common wheat introgressed from *Triticum durum*. *Acta Bot. Sin.* **46**, 867–872 (2004).
38. He, H. et al. Characterization of *Pm68*, a new powdery mildew resistance gene on chromosome 2BS of Greek durum wheat TRI 1796. *Theor. Appl. Genet.* **134**, 53–62 (2021).
39. Maccaferri, M. et al. Durum wheat genome highlights past domestication signatures and future improvement targets. *Nat. Genet.* **51**, 885–895 (2019).
40. Avni, R. et al. Wild emmer genome architecture and diversity elucidate wheat evolution and domestication. *Science* **357**, 93–97 (2017).
41. Okuyama, Y. et al. A multifaceted genomics approach allows the isolation of the rice *Pia*-blast resistance gene consisting of two adjacent NBS-LRR protein genes. *Plant J.* **66**, 467–479 (2011).
42. Guo, G. et al. The wheat NLR pair RXL/Pm5e confers resistance to powdery mildew. *Plant Biotechnol. J.* **23**, 1260–1276 (2025).
43. Williams, S. J. et al. An autoactive mutant of the M flax rust resistance protein has a preference for binding ATP, whereas wild-type M protein binds ADP. *Mol. Plant Microbe Interact.* **24**, 897–906 (2011).
44. Zdrzalek, R., Kamoun, S., Terauchi, R., Saitoh, H. & Banfield, M. J. The rice NLR pair Pikp-1/Pikp-2 initiates cell death through receptor cooperation rather than negative regulation. *PLoS One* **15**, e0238616 (2020).
45. Cavalet-Giorsa, E. et al. Origin and evolution of the bread wheat D genome. *Nature* **633**, 848–855 (2024).
46. Adhikari, L. et al. Dissecting the population structure, diversity and genetic architecture of disease resistance in wild emmer wheat (*Triticum turgidum* subsp. *dicoccoides*). *Res. Square* https://doi.org/10.21203/rs.3.rs-4909521/v1 (2024).
47. Avni, R. et al. Ultra-dense genetic map of durum wheat x wild emmer wheat developed using the 90K iSelect SNP genotyping assay. *Mol. Breed.* **34**, 1549–1562 (2014).
48. Yang, Z. E. A. Two complementary NLRs from wild emmer wheat confer powdery mildew resistance. *Nat. Commun.* xx: xxx (2024).
49. Jones, J. D. G., Staskawicz, B. J. & Dangl, J. L. The plant immune system: from discovery to deployment. *Cell* **187**, 2095–2116 (2024).
50. Adachi, H., Derevnina, L. & Kamoun, S. NLR singletons, pairs, and networks: evolution, assembly, and regulation of the intracellular immunoreceptor circuitry of plants. *Curr. Opin. Plant Biol.* **50**, 121–131 (2019).
51. Salcedo, A. et al. Variation in the *AvrSr35* gene determines *Sr35* resistance against wheat stem rust race Ug99. *Science* **358**, 1604–1606 (2017).
52. Wang, J. Z. et al. Ligand–triggered allosteric ADP release primes a plant NLR complex. *Science* **364**, eaav5868 (2019).
53. Wang, J., et al. Reconstitution and structure of a plant NLR resistosome conferring immunity. Science **364**, eaav5870 (2019).
54. Yuan, B. et al. The *Pik-p* resistance to Magnaporthe oryzae in rice is mediated by a pair of closely linked CC-NBS-LRR genes. *Theor. Appl. Genet.* **122**, 1017–1028 (2011).
55. Césari, S. et al. The NB-LRR proteins RGA4 and RGA5 interact functionally and physically to confer disease resistance. *EMBO J.* **33**, 1941–1959 (2014).
56. Gerechter-Amital, Z. K. & Grama, A. Inheritance of resistance to stripe rust (*Puccinia striformis*) in crosses between wild emmer (*Triticum dicoccoides*) and cultivated tetraploid and hexaploid wheats. I. *Triticum durum*. *Euphytica* **23**, 387–392 (1974).
57. He, H. et al. Comparative mapping of powdery mildew resistance gene *Pm21* and functional characterization of resistance-related genes in wheat. *Theor. Appl. Genet.* **129**, 819–829 (2016).
58. An, D. et al. Molecular cytogenetic characterization of a new wheat-rye 4R chromosome translocation line resistant to powdery mildew. *Chromosome Res.* **21**, 419–432 (2013).
59. Li, Y. et al. Intracellular reactive oxygen species-aided localized cell death contributing to immune responses against wheat powdery mildew pathogen. *Mol. Physiol. Plant Pathol.* **113**, 884–892 (2023).
60. Cheng, H. et al. Haplotype-resolved assembly of diploid genomes without parental data. *Nat. Biotechnol.* **40**, 1332–1335 (2022).
61. Shen, W., Le, S., Li, Y. & Hu, F. Q. SeqKit: a cross–platform and ultrafast toolkit for FASTA/Q file manipulation. *PLoS One* **11**, e0163962 (2016).
62. Bolger, A. M., Marc, L. & Bjoern, U. Trimmomatic: a flexible trimmer for Illumina sequence data. *Bioinformatics* **30**, 2114–2120 (2014).
63. Zhang, Z. et al. Dispersed emergence and protracted domestication of polyploid wheat uncovered by mosaic ancestral haploblock inference. *Nat. Commun.* **13**, 3891 (2022).
64. Wang, H. et al. Sympatric speciation of wild emmer wheat driven by ecology and chromosomal rearrangements. *Proc. Natl. Acad. Sci. USA* **117**, 5955–5963 (2019).
65. Cheng, H. et al. Frequent intra- and inter-species introgression shapes the landscape of genetic variation in bread wheat. *Genome Biol.* **20**, 136 (2019).
66. Wang, Y. et al. Molecular evidence for adaptive evolution of drought tolerance in wild cereals. *N. Phytol.* **237**, 497–514 (2023).
67. Abramson, J. et al. Accurate structure prediction of biomolecular interactions with AlphaFold 3. *Nature* **630**, 493–500 (2024).

68. Livak, K. J. & Schmittgen, T. D. Analysis of relative gene expression data using real-time quantitative PCR and the $2^{-\Delta\Delta Ct}$ method. *Methods* **25**, 402–408 (2001).
69. Zhang, S. et al. Targeted mutagenesis using the *Agrobacterium tumefaciens*–mediated CRISPR–Cas9 system in common wheat. *BMC Plant Biol.* **18**, 302 (2018).
70. Higuchi, R., Krummel, B. & Saiki, R. K. A general method of in vitro preparation and specific mutagenesis of DNA fragments: study of protein and DNA interactions. *Nucleic Acids Res.* **16**, 7351–7367 (1988).
71. Gao, A. et al. Pm21 CC domain activity modulated by intramolecular interactions is implicated in cell death and disease resistance. *Mol. Plant Pathol.* **21**, 975–984 (2020).

Acknowledgements

This study was supported by grants from National Natural Science Foundation of China (32171990 to H.H.), Natural Science Foundation of Jiangsu Province (BK20231321 to H.H.; BK20240839 to J.W.), Key Technology R&D Program of Henan Province of China (241111110900, 231111112900 and 225200810024 to A.G.), State Key Laboratory of Plant Cell and Chromosome Engineering (PCCE-KF-2022-07 to S.Z.), State Key Laboratory of Crop Biology in Shandong Agricultural University (2021KF01 to H.H.), Start-up funding of Center for Excellence in Molecular Plant Sciences, Chinese Academy of Sciences (to Y.W.), Project of the Faculty of Agricultural Engineering of Jiangsu University (NZXB20200102 to C.W.) and Key and General Projects of Jiangsu Province (BE2022338 to C.W.). The authors thank the Genebank Information System of the IPK Gatersleben (GBIS-IPK), the U.S. National Plant Germplasm System (NPGS), the Chinese Crop Germplasm Resources Information System (CCGRIS), Dr. Zhiyong Liu (Institute of Genetics and Developmental Biology, Chinese Academy of Sciences, Beijing, China) and Dr. Hao Li (Henan University, Kaifeng, China) for providing durum wheat and wild emmer accessions, Dr. Genying Li (Crop Research Institution, Shandong Academy of Agricultural Sciences, Jinan, China) for providing the binary vector pLGY02, Dr. Yinghui Li (Triticeae Research Institut, Sichuan Agricultural University, Chengdu, China) for assistance of powdery mildew resistance spectrum analysis, Yi Ouyang (Center for Excellence in Molecular Plant Sciences, Chinese Academy of Sciences, Shanghai, China) for protein structure modeling and Dr. Li Wan (Center for Excellence in Molecular Plant Sciences, Chinese Academy of Sciences, Shanghai, China) for advice on the discussion of NLR immune receptors.

Author contributions

H.H., A.G., and Y.W. conceived and designed the research. H.H., Q.T., Q.Z., S.Z., S.L., Y.B., J.L.W., J.W., and H.X. performed experiments. H.H., J.L., Y.W., E.C.-G., S.G.K., C.W., and A.G. analyzed the data. H.H., H.L., A.G., and Y.W. wrote the manuscript.

Competing interests

The authors declare no competing interests.

Additional information

Supplementary information The online version contains supplementary material available at https://doi.org/10.1038/s41467-025-64048-z.

Correspondence and requests for materials should be addressed to Huagang He, Anli Gao or Yajun Wang.

Peer review information *Nature Communications* thanks Adachi Hiroaki, Javier Sánchez-Martín and the other, anonymous, reviewer(s) for their contribution to the peer review of this work. A peer review file is available.